# On the Application of the IMOMO (Integrated Molecular Orbital + Molecular Orbital) Method

**THOM VREVEN,* KEIJI MOROKUMA**

*Cherry L. Emerson Center for Scientific Computation and Department of Chemistry, Emory University, Atlanta, Georgia 30322*

*Received 3 May 2000; accepted 13 June 2000*

**ABSTRACT:** Five years ago Morokuma and colleagues introduced the IMOMO method, which integrates two molecular orbital methods into one calculation. Since then, the method has been expanded in several ways; it has been generalized to consider up to three methods, and has been unified as the ONIOM method to include both MO and MM combinations. In this review we present the history of the method, a number of chemical problems that we have studied, how to assess IMOMO combinations and partitionings, and our latest efforts that take the method beyond the conventional investigation of ground state energy surfaces. In particular, we emphasize the importance of the *S*-value test for validation of the ONIOM method/model combinations. The method combination depends much on the properties and accuracies required. Generally speaking, however, if the target level is CCSD(T) or G2, the best choice of low level is MP2. If MP2 or DFT is the target level, HF or eventually semiempirical MO methods are good choices of low level. These methods can be further combined with an outer-most layer of the MM level. © 2000 John Wiley & Sons, Inc. J Comput Chem 21: 1419–1432, 2000

**Keywords:** IMOMO method; molecular orbital methods; ONIOM method; hybrid method

*Present address: Gaussian, Inc., 140 Washington Ave., North Heaven, CT 06473

*Correspondence to:* K. Morokuma; e-mail: morokuma@euch4e.chem.emory.edu

Contract/grant sponsor: National Science Foundation; contract/grant number: CHE-9627775

## Introduction

The main disadvantage of accurate quantum chemical methods is that the computational cost scales extremely unfavorably with the size of the system. High correlation methods, such as CCSD(T),[1] scale to the fifth or sixth power, as do model chemistries that are based upon these methods, such as G2[2] or CBS.[3] Of course, methods that scale more favorably are available, but there will always remain a struggle between accuracy and computational feasibility. Fortunately, the efficiency of computational methods has greatly improved in recent years, and especially linear scaling[4] density functional theory (DFT)[5] allows the accurate study of very large systems. However, these methods are still "conventional" in the sense that the entire system is treated uniformly with the same accuracy. Local correlation methods[6] improve the efficiency in a different way, and are based on the assumption that different accuracies are required for different regions of the system. An example is the reaction center in a bond breaking process. However, all the methods mentioned above share an important feature, being that one calculation is performed for the entire system.

A second approach to improve the computational efficiency is to use different methods for different parts of the system. Most of these so-called hybrid methods combine quantum chemical methods with molecular mechanics methods, often referred to as QM/MM, and have proven very successful.[7] The *integrated molecular orbital + molecular mechanics* method (IMOMM), which integrates MO methods with the MM3 force field,[8] was independently developed by Morokuma and colleagues, and has a philosophy slightly different from QM/MM.[9] Soon afterward, it was realized that the extrapolation scheme in IMOMM can be generalized to combine two quantum chemical methods as well. This resulted in a combined MO+MO method, which was referred to as *integrated molecular orbital + molecular orbital* method (IMOMO).[10] Later the integration of more than two methods was accomplished, and the entire suit of integrated methods was named the ONIOM method (*our own n-layered integrated molecular orbital + molecular mechanics method*).[11] Thus, IMOMO encompasses both two-layered ONIOM2(MO:MO) and three-layered ONIOM3(MO:MO:MO), and IMOMM is, in principle, equivalent to ONIOM2(MO:MM) and ONIOM3(MO:MO:MM). However, it must be noted that between the various versions there are some subtle differences in practical implementation, which will be discussed below. The latest incarnation of ONIOM is available in Gaussian98, and can integrate up to three layers of most electronic structure methods and/or molecular mechanics methods from the package.[12] Because this is technically not an easy feat, some methods are currently incompatible, and improvement of the program's reliability is a continuing effort. More information on the ONIOM program, including problems one may encounter, will be available via the internet site of our group at Emory University.[13]

In the present review, we will emphasize the integration of only the MO methods, namely, IMOMO, or ONIOM2(MO:MO) and ONIOM3(MO:MO:MO). Integration of different MO methods is quite a unique feature of the ONIOM method, unavailable in any other hybrid method. The application of the IMOMM method has been reviewed before and will not be part of this article.[14] Furthermore, the ONIOM method, both IMOMO and IMOMM, also received attention in the Encyclopedia of Computational Chemistry.[15]

## Theory

In the two-layered ONIOM method, the total energy of the system is obtained from three independent calculations:

$$E^{\mathrm{ONIOM2}} = E^{\mathrm{high}}_{\mathrm{model}} + E^{\mathrm{low}}_{\mathrm{real}} - E^{\mathrm{low}}_{\mathrm{model}}, \qquad (1)$$

where *real* denotes the full system, which is treated at the *low* level, while *model* denotes the part of the system of which the energy is calculated at both the *high* and *low* level. The concept of ONIOM method is represented schematically in Figure 1. One can see that the method can be regarded as an extrapolation scheme. Starting from $E^{\mathrm{low}}_{\mathrm{model}}$, the extrapolation to the high-level calculation ($E^{\mathrm{high}}_{\mathrm{model}} - E^{\mathrm{low}}_{\mathrm{model}}$) and the extrapolation to the real system ($E^{\mathrm{low}}_{\mathrm{real}} - E^{\mathrm{low}}_{\mathrm{model}}$) are assumed to give an estimate for $E^{\mathrm{high}}_{\mathrm{real}}$. For a three-layer ONIOM scheme, the energy expression can be written as

$$E^{\mathrm{ONIOM3}} = E^{\mathrm{high}}_{\mathrm{small\ model}} + E^{\mathrm{medium}}_{\mathrm{intermediate\ model}} - E^{\mathrm{medium}}_{\mathrm{small\ model}} + E^{\mathrm{low}}_{\mathrm{real}} - E^{\mathrm{low}}_{\mathrm{intermediate\ model}} \qquad (2)$$

Although ONIOM can in principle be used for any number ($N$) of layers, for which $2N - 1$ subcalculations are required, the implementation in the Gaussian98 package is currently restricted to three.

The definition of the model system is rather straightforward when there is no covalent bond between the layers. If one considers a solute molecule

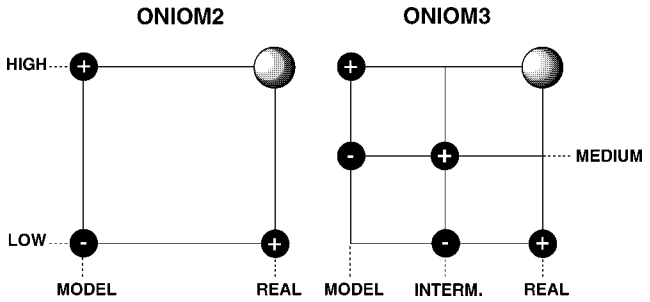


**FIGURE 1.** Schematic representation of the two- and three-layer ONIOM extrapolation scheme.

solvated with one solvent molecule as the *real* system, the solute will be the *model* system, and the solute–solvent interaction is naturally included in the *low* level calculation of the *real* system. The situation becomes more complicated when covalent bond exists between the layers. The calculation on the real system does not pose any problems, but what can we use as model system? Simply cutting the bonds would result in a model system with dangling bonds, and its electronic structure would be very different from the real system. The most straightforward way to ensure that the model system is representative for the real system is to saturate the dangling bonds with *link atoms*, which is the scheme chosen for our ONIOM methods. For example, if a methyl group is treated at the low level, this group can be substituted by a hydrogen atom in the model system. One chooses link atoms that best mimic the substituents that exist only in the real system. In practice, hydrogen atoms are good link atoms when carbon–carbon bonds are broken, but in some cases other atoms may be better.[16] One may also shift the one-electron energy of the link atom with a shift operator to mimic the electronegativity of the replaced atom,[17] although we have not explored its usefulness in ONIOM in detail. Several alternative schemes to connect the regions have been investigated by other groups, mostly within the QM/MM framework. These developments involve orbitals instead of link atoms,[18] a region between the QM and MM region that allows charge transfer,[19] link atoms that better mimic the groups they substitute,[20] and so forth. Most of these schemes could be used in our ONIOM method. However, one of the most attractive features of ONIOM is that it is completely general; any pair or trio of methods available in the Gaussian package can be combined. Some of these link schemes are specific to a certain electronic structure method, which would compromise this generality.

Although this overview centers on the integration of two or three MO methods, we do want to spend a few lines to place our ONIOM(MO:MM) method in the general field of hybrid MO+MM or QM/MM methods. First, we feel the ONIOM (MO:MM) implementation in Gaussian is very general, similar to ONIOM(MO:MO). This must not be confused with functionality of the implementation. So far, only three MM force fields have been implemented in Gaussian, and many types of MM force fields that are common in other QM/MM packages are not (yet) available. Second, a feature absent in other QM/MM methods, is the integration of two MO levels with one MM level, ONIOM3 (MO:MO:MM). On the other hand, the ONIOM (MO:MM) scheme has also a disadvantage when strictly applied. The interaction between the MO and MM regions is only treated at present at the MM level, which was referred to by Bakowies and Thiel as mechanical embedding.[22] An alternative in QM/MM methods is the inclusion of the charge distribution of the MM region, which consists usually out of the MM atom charges, in the QM Hamiltonian. This accounts for a more accurate description of the electrostatic interaction between the two regions, and allows the QM wave function to be polarized. Bakowies and Thiel referred to this scheme as electronic embedding. Although the current implementation in Gaussian can only consider mechanical embedding, we are extending the method facilitate both types of embedding.

Based on the theoretical framework of the ONIOM method, we can comment on the practical implementation in the Gaussian package and how this relates to the performance. From the preceding paragraphs we know that the ONIOM2 energy is composed out of the energies of three well-defined systems. In fact, when an ONIOM calculation is requested, Gaussian automatically executes three subcalculations, or five subcalculations in the case of ONIOM3, followed by the integration of the results

to obtain the ONIOM values. These subcalculations are completely independent, and the ONIOM routines in the package can therefore be regarded as a set of drivers that construct the model system(s), execute the standard electronic structure programs, and finally combine the results. If one would construct the model system by hand, perform three (or five) separate calculations, followed by the integration according to eq. (2) or (3), the same results are obtained. The paramount advantage of this scheme is that only relatively modest modifications to the electronic structure programs were required, which ensures that any of the current of future methods available can eventually be used in the ONIOM scheme, as well as the full range of options related to each of these methods with respect to convergence and/or computational efficiency. The calculation of geometrical derivatives or other properties follows the same structure; always three or five independent standard calculations are performed, followed by the integration. The performance of the program is clear from this structure. The total calculation time is the sum of the subcalculations, while the time spend in the ONIOM subroutines is negligible. Because the cost of the low level calculation on the model system is usually negligible, the computational bottleneck in a two-layer ONIOM calculation is either the high level calculation on the model system, or the low level calculation on the real system. Which one dominates completely depends on the partitioning and method combination. With a molecular mechanics method in the low level, the high level calculation on the model system is virtually always the most time-consuming. But with a low-level method that includes electron correlation, this calculation on the real system might well be the most expensive. It must also be noted that during geometry optimizations, for each of the subcalculations, many quantities of step $n-1$ will be used for step $n$, similarly as in the standard MO method. Also the MOs of step $n-1$ are used as "guess" in step $n$. The disadvantage is that for this reason much more data must be stored on the read–write and checkpoint files than in conventional calculations, although it should never be more then three (or five) times as much. Because Gaussian is executed as a series of independent programs (or "links"), this problem does not increase the memory requirements. Finally, ONIOM(MO:MM) combinations can make use of the microiterations optimization scheme, in which a full geometry optimization for the MM part is carried out for each geometry optimization step of the MO region, which increases the efficiency significantly.[9] In conclusion, the size of problems that can be tackled with the ONIOM method is determined by the standard Gaussian program.

In the paragraphs above we considered the energy expression for the ONIOM methods, while in the next section we will discuss geometry optimization and other techniques concerned with the properties of potential energy surface. Molecular one-electron properties can also be obtained with the integrated method. An example of the calculation of properties, NMR chemical shifts, will be discussed later in this review. Several other topics on the methodology and application of IMOMO will also be discussed in detail in the next sections. These exclude examples that were merely used for demonstration purposes in the articles that documented the several phases of the IMOMO/ONIOM methodology: Organometallic systems include the oxidative addition of $H_2$ to $Pt(P(t\text{-}Bu)_3)_2$, which, in fact, was studied using an ONIOM3(MO:MO:MM) scheme,[11] the technically challenging substitution of phenyl and cyclopentadiene rings by link atoms,[16] and calculation of Pt–olefin bond energies.[16] Furthermore, the $S_N2$ reaction $Cl^- +$ alkyl chlorides,[10, 21] the epoxidation of benzene,[21] and the conformation of *n*-butane were used as test cases.[10]

## Geometry Optimization

In the construction of the ONIOM model system, atoms that belong to the high level layer have the same coordinates as the corresponding atoms in the real system. Even during geometry optimizations, these coordinates remain identical to each other. When no bond exists between the two layers, the first derivative of the energy with respect to the geometry is easy to obtain.

$$\frac{\partial E^{\mathrm{ONIOM}}}{\partial \mathbf{q}} = \frac{\partial E^{\mathrm{high}}_{\mathrm{model}}}{\partial \mathbf{q}} + \frac{\partial E^{\mathrm{low}}_{\mathrm{real}}}{\partial \mathbf{q}} - \frac{\partial E^{\mathrm{low}}_{\mathrm{model}}}{\partial \mathbf{q}} \qquad (3)$$

However, the link atoms used in the model system do not exist in the real system, and one of the main issues in this type of hybrid methods is their geometrical placement. There are a number of possibilities, of which several have been used in hybrid methods. We will now briefly discuss some of the options and associated problems.

The simplest scheme would be to have independent coordinates for the link atoms. Thus, the number of degrees of freedom would increase with six times the number of links between the high and low level layers (not three times the number of links, because a link atom does not need to have the same

coordinates in the high and low level calculations on the model system). This scheme is not very attractive, because in the hybrid calculation there are more degrees of freedom than in the conventional calculation, and therefore, the potential energy surface is not uniquely defined. One could solve this problem by always optimizing the position of the link atoms in geometry optimizations, but this will not be straightforward in anything else than equilibrium optimization. A second problem is that now the link atoms in the model system will always be at equilibrium positions, while in fact, steric effects may cause the replaced substituents to have very different orientations. Third, the model system at the high level will not be the same as the model system at the low level.

A better choice is to connect the link atoms to the high level layer with the same angular and dihedral values as the link atom hosts (LAHs, the atoms replaced by the link atoms in the model system) in the real system. Now steric effects of the substituents are also taken into account in the two model system calculations. The remaining problem is which bond lengths to use between the link atom and the high level layer. Optimizing the bond lengths for the each model system separately yields again different model systems for the high and low level. An alternative is to constrain the bond lengths to have the same value in the two calculations. This, however, is likely to result in bond collapsing.[22] In IMOMM, our first implementation of the hybrid method, this problem was circumvented by using fixed (standard) bond lengths between the link atoms and the high level layer, as well as fixed bond lengths between the LAH atoms and the high level layer. This scheme works fine for geometry optimization. However, in this scheme, one degree of freedom is lost for each link between the high and low level layers, which causes problems with, for example, dynamics or frequency calculations.

The bond collapsing problem was approached in a different way by Corchado and Truhlar, who included a harmonic term in the IMOMO energy expression [eq. (4)]. This term ensures the bond length to remain physically reasonable.[23] However, the scheme, referred to as *Integrated Molecular Orbital with Harmonic Cap* (IMOHC), still yields a modified number of degrees of freedom. Also, the angular and dihedral parameters of the link atoms can collapse or yield unreasonable values (provided they are not constrained, as in the IMOMM scheme outlined above), which can be prevented by introducing harmonic terms for the angles and dihedrals as well.

$$E^{\mathrm{IMOHC}} = E^{\mathrm{low}}_{\mathrm{real}} - E^{\mathrm{low}}_{\mathrm{model}} + E^{\mathrm{high}}_{\mathrm{model}} + C(R_{\mathrm{link}} - R_{\mathrm{equilibrium}})^2 \quad (4)$$

Our Gaussian98 implementation of the link atom in the ONIOM method yields the correct number of degrees of freedom.[16] The angles and dihedrals are treated in the same manner as in the IMOMM scheme, while the bond distances between the high level layer and the link atoms are obtained by scaling the corresponding distances between the high level layer and the LAH atoms: $\mathbf{R}_{\mathrm{link}} = \mathbf{R}_{\mathrm{high\ level\ atom}} + g(\mathbf{R}_{\mathrm{LAH}} - \mathbf{R}_{\mathrm{high\ level\ atom}})$, where $R_{\mathrm{high\ level\ atom}}$ denotes the atom in the high level layer to which the link atom is connected. The scaling factor $g$ is chosen so that reasonable bond lengths between the LAH atoms and high level layer atoms yield also reasonable bond lengths between the link atoms and high-level layer atoms. In this version, the correct number of degrees of freedom ensures the potential energy surface to be well defined, and gradients and higher derivatives are available. In this case, one must use the Jacobian $\mathbf{J}$ to convert the coordinate system for the model system to the coordinate system for the real system.

$$\frac{\partial E^{\mathrm{ONIOM}}}{\partial \mathbf{q}} = \frac{\partial E^{\mathrm{high}}_{\mathrm{model}}}{\partial \mathbf{q}} \cdot \mathbf{J} + \frac{\partial E^{\mathrm{low}}_{\mathrm{real}}}{\partial \mathbf{q}} - \frac{\partial E^{\mathrm{low}}_{\mathrm{model}}}{\partial \mathbf{q}} \cdot \mathbf{J} \quad (5)$$

The Hessian or higher order derivatives can be defined uniquely in a similar fashion. Any method for the investigation of potential energy surfaces available for conventional methods can now be used for the ONIOM method. For example, the first IMOMO dynamics studies are currently in progress.

## Bond Dissociation Energies

IMOMO methods can be applied to virtually any chemical problem, but one of the first areas that has been covered in great detail is the calculation of bond dissociation energies (BDEs). Besides several papers in which BDEs were used as illustration of the method,[16, 21] a number of studies have focused exclusively on this topic. Truhlar and Coitiño considered the hydrogen dissociation from single and doubly substituted (F, Cl, OH, and $NH_2$) ethane[24–26] and methane.[26] In these studies, high correlation methods were used for the part of the system where the dissociation takes place, while HF or a lower correlation method was used for the remainder of the system. The authors referred to this specific partitioning and method combination as *correlated capped*

**TABLE I.**
**Bond Dissociation Energies (kcal/mol) Using a Minimal Model.**

| Reaction[a] | ref.[b] | Experimental | G2MS(R):RMP2[c] | G2MS(U):RMP2[c] |
|---|---|---|---|---|
| Ph—F | I | 125.7 ± 2 | 124.6 | 125.2 |
| Ph—$CH_3$ | I | 101.8 ± 2 | 100.3 | 101.9 |
| $PhSiH_2$—H | I | 88.2 | 86.3 | 86.3 |
| $PhCH_2$—$SCH_3$ | I | 61.4 ± 2 | 61.6 | 62.4 |
| $F_5SO$—$OSF_5$ | I | 37.2 ± 2 | 37.3 | 37.7 |
| $PhCH_2$—H | II | 88.0 ± 1 | 90.1 | 90.4 |
| MePhCH—H | II | 85.4 ± 1.5 | 87.8 | 88.2 |
| $Me_2PhC$—H | II | 84.4 ± 1.5 | 87.2 | 87.6 |
| $Ph_2CH$—H | II | 84 ± 2 | 82.6 | 82.9 |
| $MePh_2C$—H | II | 81 ± 2 | 82.6 | 82.9 |
| $Ph_3C$—H | II | n.a. | 75.9 | |
| $PhCH_2$—$CH_3$ | II | 75.8 ± 1 | 79.0 | 79.7 |
| MePhCH—$CH_3$ | II | 74.6 ± 1.5 | 78.1 | 78.9 |
| $Me_2PhC$—$CH_3$ | II | 73.7 ± 1.5 | 77.2 | 77.9 |
| $Ph_2CH$—$CH_3$ | II | 72 ± 2 | 72.7 | 73.5 |
| $MePh_2C$—$CH_3$ | II | 69 ± 2 | 72.9 | 73.6 |
| $Ph_3C$—$CH_3$ | II | n.a. | 64.1 | |
| | | | G2MS(R):RMP2:RHF[d] | |
| $C_{60}$: $S_0 \rightarrow T_1$ ($\pi$ bond) | III | 36.1 | 35.1 | |
| | | | G2MS(R):RMP2:B3LYP[e] | |
| $Ph_3C$—$CPh_3$ | IV | n.a. | 16.4 | |

See references for specific procedures and origin of experimental data.
[a] The dissociation bond is indicated by the dash.
[b] I from Froese et al.,[27] II from Vreven et al.,[29] III from Froese et al.,[28] IV from Vreven et al.[30]
[c] Geometries and frequencies from B3LYP, 6-31G(d) basis set employed for the MP2 calculations.
[d] Geometry from AM1, no ZPE correction, intermediate model is naphthalene.
[e] 6-31G basis set for B3LYP, geometry obtained at ONIOM2(B3LYP/6-31G:B3LYP/3-21G) level; see Figure 2 for partitioning.

*subsystem*, or CCSS. Several aspects of the method were investigated. In the first article, the low level was always HF, and a variety of methods [MP4SDQ, CCSD, and QCSD(T)] were tested for the high level.[26] In the second article, the dependence on the basis sets and low level method was investigated,[24] while in the third study a larger variety of electronic structure methods was considered.[25]

The dissociation energies of sets of larger molecules were calculated by Froese[27, 28] and Vreven.[29, 30] In both studies, a number of high and low levels were investigated, but the geometries and zero-point vibrational energies or temperature corrections were obtained at the nonintegrated B3LYP level. In most cases, a minimal model was employed (only the non-H atoms in the dissociation fragment), and the results show that the G2MS:RMP2 combination yields BDEs very close to the experimental values (G2MS[31] is our own inexpensive G2-like method, G2MS(R/U) = CCSD(T)/6-31G(d) + (R/U)OMP2/6-311+G(2df,2p) − (R/U)OMP2/6-31G(d), which we have used extensively in our IMOMO studies). In Table I we show the molecules from these studies that contain more than six non-H atoms. The error with the experimental values is usually not more than a few kcal/mol, and could probably be reduced further by fine tuning the choice of basis sets. The primary conclusion is that a very high correlation method is required for the reaction center, but a low level correlation method is still needed for the remainder of the system. Spin-contamination in the low-level method is an important problem for molecules containing aromatic substituents, and therefore, unrestricted methods proved inappropriate. We were able to predict the BDE for $Ph_3C$—H and $Ph_3C$—$CH_3$, for which the experimental values are not available.

The last two entries in Table I, $C_{60}$ fullerene and hexaphenylethane (HPE), are systems too large for the G2MS:MP2 calculation, and it was necessary

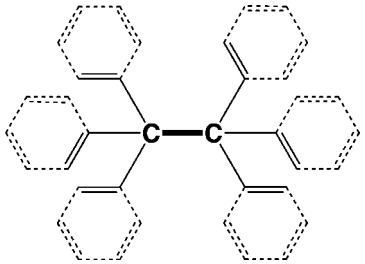

**FIGURE 2.** Partitioning used in the ONIOM3 calculation of the bond dissociation energy of hexaphenylethane (HPE). Layer I consists of the bold C—C atoms (and terminating H atoms), and layers II and III are drawn with solid lines and broken lines, respectively. The geometry optimizations have been carried out with ONIOM2(B3LYP/6-31G:B3LYP/3-21G), where the 6-31G basis set was used for layers I and II, and the 3-21G basis sets for layer III. The energy calculations were carried out with ONIOM3(G2MS(R):RMP2/6-31G(d):B3LYP/3-21G).

to introduce a third layer treated at a less expensive level. In the case of $C_{60}$, RHF for the lowest level proved useful, and for HPE B3LYP was a good choice. In Figure 2 we show the partitioning that was used in the HPE calculations, which will be discussed in a forthcoming article.[30] The HPE example is particularly interesting. This compound is thought to be too unstable to exist,[32] but our BDE value suggests that synthesis could be possible.

## Diels–Alder Reactions

Besides bond dissociation energies, Diels–Alder reactions have been studied extensively with the IMOMO method. In the article that first defined the ONIOM method, we discussed the addition of acrolein to substituted 1,3-butadienes,[11] where the ethylene–butadiene system was used as the model system. It is expected that the electronic effect of the COH group in acrolein also needs to be treated with an MO method (MM is incapable of treating the electronic effects), and it was therefore included at an intermediate layer. The alkyl substituents on butadiene are not expected to play an important role, and were treated at a third, low-accuracy level. Both the optimization and energy calculation were performed with a variety of combinations. The ONIOM(B3LYP:HF:MM3) combination (the 6-31G basis set has been used throughout) yields a deviation in the activation barrier of only 1.4 kcal/mol from the B3LYP target, for both the reaction of acrolein with isoprene (2-methyl-1,3-butadiene), and the reaction of acrolein with 2-*tert*-butyl-1,3-butadiene. The third reaction studied, ethylene + *s-trans trans,trans*-1,4-di-*tert*-butyl-1,3-butadiene, with MP4 as target method, yields good results with the ONIOM(MP4:MP2:MM3) combination. The error in activation energy is 2.3 kcal/mol, which is significantly less than the 4.4 kcal/mol error for MP4:HF:MM3. This is similar to the IMOMO studies of bond dissociation energies, where we observed that often results are not adequate when the HF level is employed for a layer too close to the reaction center.

The second investigation of Diels–Alder reactions was reported in the article that introduced G2MS,[31] our less costly alternative for the G2 method.[2] The IMOMO(G2MS:MP2)//B3LYP + ZPE(B3LYP) combination was very successful, and two subsequent IMOMO studies of Diels–Alder reactions focussed on this combination.[33, 34] Because G2MS calculations are too expensive for systems with more than eight non-H atoms, the method was tested by comparing the results directly to experimental values. In Table II, we summarize the IMOMO(G2MS:MP2) results for Diels–Alder reactions for which experimental activation energies are available. The computational data is in fairly good agreement with the experimental values. In Table III, we show the branching ratio of several reactions. The results not always agree quantitatively with the experimental values, which is the result of the branching ratio being very sensitive to small errors in our calculated energetics. However, IMOMO(G2MS:MP2) reproduces qualitative

**TABLE II.**
**Experimental and IMOMO(G2MS:MP2) Activation Barriers (kcal/mol) for Diels–Alder Reactions.**

| | G2MS:MP2 | Exp. |
|---|---|---|
| Butadiene + butadiene | 23.5 | 23.7 ± 0.2, 24.5 |
| Acrolein + isoprene | 17.6 | 18.7 |
| Maleic anhydride + isoprene | 9.2 | 12.2 |
| Maleic anhydride + 2-*tert*-butyl-1,3-butadiene | 4.6 | 6.5 |

**TABLE III.**
**IMOMO(G2MS:MP2) and Experimental (in Parentheses) Branching Ratios in Diels–Alder Reactions.**

| Reactants | Product Ratios | | | |
|---|---|---|---|---|
| | 1, 2, *cis* | 1, 2, *trans* | 1, 3, *cis* | 1, 3, *trans* |
| Acrylic acid + 2,4-pentadienoic acid | 75.5 (61) | 22.9 (22) | 0.9 (9) | 0.7 (8) |
| | *syn* | *anti* | | |
| Ethylene + **1** | 99.9 (93) | 0.1 (7) | | |
| Acetylene + **1** | 7.2 (8) | 92.8 (92) | | |

well the reversal of *syn/anti* reactivity for ethylene and acetylene with **1**, which is caused by the repulsion between the lone pair of oxygen in **1** with the $\pi$-orbitals of acetylene in the *syn* transition state (Scheme 1).

## The *S*-Value Test

The most critical question when using the ONIOM scheme is how to select the methods that will be combined, and the partitioning of the system into high and low level layers. These two factors are closely related. When using the ONIOM method, at first one has to decide the high-level method. Then the *high*-level calculation for the *real* system is the *target* calculation that one attempts to approach with the ONIOM method. The ONIOM results converge to the target results when the low level method approaches the high level, or when the size of the model system approaches the real system. Thus there are two ways to improve the ONIOM results, both of which should be considered.

How can one select the appropriate computational levels and size of the model system? It very much depends on the properties one is interested in and the errors one can tolerate in the ONIOM extrapolation. Unfortunately, the studies reported so far only cover a small number of chemical problems, so it is unlikely that the problem of interest is among those. The first rule of thumb is that if one knows by intuition who are the major players and who are the minor players, include the major players in the model system to be treated at high level, while the minor players can be treated only at low level in the real system. For instance, if one is interested in chemical reactions in solvated cluster (the real system), the reactants (and solvent molecules directly involved in the reaction) will constitute the model system. However, in some cases, one cannot identify major players. For example, for the equilibrium structure of $HCl(H_2O)_4$ shown in Figure 3 studied by Re et al.,[35] the relative energies of one neutral complex structure (A) and two ion-pair structures (B and C) at ONIOM(B3LYP/D95++(d,p):BLYP/D95+(d)) (HCl at high level and water molecules at low level) do not agree with either the high or low level ordinary MO results. A detailed analysis[35] shows that the interaction energy in these clusters consists of the sum/difference of large two-, three-, and multibody terms, and relatively small errors introduced by ONIOM in individual terms accumulate and easily wipe out the small (~4 kcal/mol) difference in the total binding energy among difference structures.

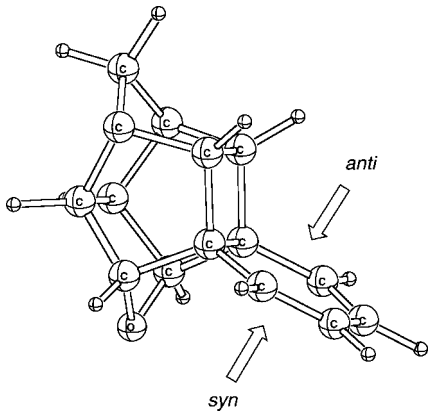


**SCHEME 1.**

We have abundant experience with the study of bond dissociation, for which it is clear which ONIOM schemes to use.[24–30] When an appropriate combination is not available from previous studies, chemical intuition, combined with trial and error, can be used to obtain schemes that agree with experimental data. A good example of such a procedure is given for the bond energies in $C_{60}$.[28] A problem with this strategy is that the low level method in ONIOM calculations often plays a role very different from if

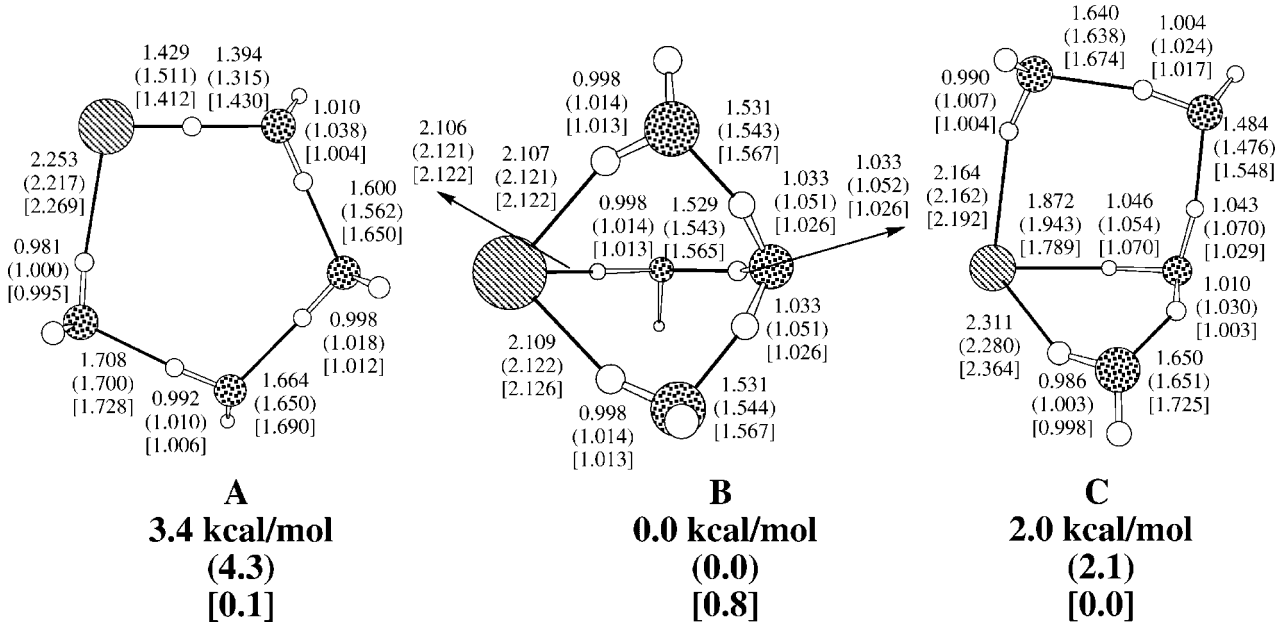


**FIGURE 3.** The optimized structures (in Å) and relative energies (in kcal/mol) of three forms of $(HCl)(H_2O)_4$ at B3LYP/D95++(d,p), BLYP/D95+(d) (in parentheses) and ONIOM(B3LYP/D95++(d, p) : BLYP/D95+(d)) (in brackets; the model system is $(HCl)(H_2O)$) level.

it were a stand-alone method, and it can therefore be difficult to use intuition to find the appropriate method. Furthermore, the number of possibilities (based on computational levels and partitioning) increases exponentially when the system becomes larger and a three or higher layer integrated method is employed. A more direct way of finding an appropriate ONIOM method is preferred.

A systematic way of finding a correct ONIOM combination is by virtue of the substituent-value test, or *S-value test*, which we have used in several of our recent ONIOM studies. Take, for instance, a relative energy $\Delta E$, such as bond energy or activation energy. The *S*-value for a certain level is defined as the difference of $\Delta E$ between the real and the model system.

$$\Delta S^{\text{level}} = \Delta E^{\text{level}}_{\text{real}} - \Delta E^{\text{level}}_{\text{model}} \tag{6}$$

i.e., the "substituent effect" on $\Delta E$ at a given level, as shown in Scheme 2. Using the $\Delta S$ values, the error $D$ of the ONIOM extrapolation $\Delta E^{\text{ONIOM}}$, compared to the target calculation $\Delta E^{\text{high}}_{\text{real}}$, can be written as:

$$\begin{aligned}\Delta D &= \Delta E^{\text{high}}_{\text{real}} - \Delta E^{\text{ONIOM}} \\ &= \left(\Delta E^{\text{high}}_{\text{real}} - \Delta E^{\text{high}}_{\text{model}}\right) - \left(\Delta E^{\text{low}}_{\text{real}} - \Delta E^{\text{low}}_{\text{model}}\right) \\ &= \Delta S^{\text{high}} - \Delta S^{\text{low}}\end{aligned} \tag{7}$$

If the $\Delta S$ value at the low level is the same as the $\Delta S$ value at the high level, the ONIOM method exactly reproduces the target method.

How can the *S*-value test be used in practice? Generally, one attempts to use the ONIOM method to reproduce a target level of calculations for a series of compounds. Obtaining the $\Delta S^{\text{high}}$ value is nothing but performing the high level calculation for the real system one was trying to avoid. The idea of the *S*-value test is to calculate $\Delta S$ values at various levels, including the level one wants to use as the high level, only for a test set, which is a number of the smaller compounds. These $\Delta S^{\text{high}}$ values can then be compared to the $\Delta S$-values for a variety of potential low levels, and the method closest to the $\Delta S^{\text{target}}$ values will yield the most accurate ONIOM results. Thus, using a small test set, the ONIOM combina-

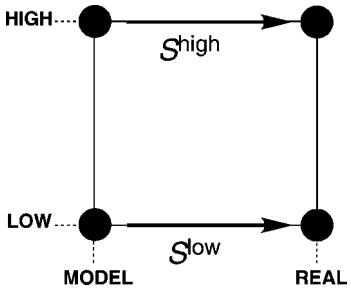


**SCHEME 2.**

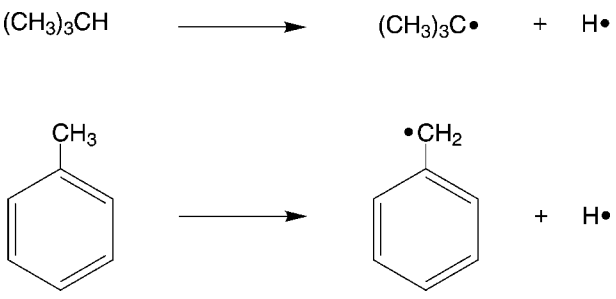


**SCHEME 3.**

tion can be calibrated, and subsequently be used to investigate the systems of interest. Of course, the *S*-value test is only possible when calculations of a representative set can be performed at the target level.

Let us consider as example the hydrogen atom dissociation from *iso*-butane and toluene, as shown in Scheme 3, which comes from a more extensive set reported by the authors.[29] The geometries are obtained at the B3LYP/6-31G level, and the minimal model system (methane) has been employed. In Table IV we show the $\Delta S$ values for the two dissociation reactions, obtained with a variety of methods [all with 6-31G(d) basis set], together with the target level G2MS(R). The $\Delta S$ values of *iso*-butane are all quite close to the target value of −7.75 kcal/mol, and from this we would conclude that we could simply choose the cheapest of the four methods as low level in ONIOM2 calculations. However, when we look at the $\Delta S$ value for toluene, a very different picture appears. Only the restricted MP2 method gives a $\Delta S$ value close enough to the target value, and it is clear that the other methods can not be used as low level to study dissociation energies of compounds including aromatic substituents. This example shows the importance of a representative set to perform the *S*-value test. Because of the importance of testing ONIOM combinations, future versions of the ONIOM program in the Gaussian package will be able to calculate the "full square" of energies, and report the resulting *S*-values.

**TABLE IV.**
**$\Delta S$ Values (kcal/mol) for Hydrogen Atom Dissociation for *iso*-Butane and Toluene, Employing a Minimal (Methane) Model and B3LYP/6-31G Geometries.**

| Level | *iso*-Butane | Toluene |
|---|---|---|
| G2MS(R) | −7.75 (0.00) | −16.21 (0.00) |
| UHF | −7.29 (+0.46) | −26.12 (−9.91) |
| RHF | −6.73 (+1.02) | −10.28 (+5.93) |
| UMP2 | −7.72 (+0.03) | +6.93 (+23.14) |
| RMP2 | −8.10 (−0.35) | −15.04 (+1.17) |

## Excited States

Although most of the IMOMO studies so far have dealt with the ground state, the method is also applicable to the investigation of higher electronic states. Froese and Morokuma reported $S_0 \rightarrow T_{1,2}$ excitation energies of cyclic alkenes and enones,[36] while current investigations of excited states include the $S_1$ isomerization of retinal protonated Schiff base models.[37]

For a two-layer ONIOM method, the energy of the excited state can be written as

$$E^{\text{ES, ONIOM}} = E^{\text{ES, low}}_{\text{real}} - E^{\text{ES, low}}_{\text{model}} + E^{\text{ES, high}}_{\text{model}} \quad (8)$$

We can distinguish two cases in the study of excited states using the ONIOM method. First, when the excitation is sufficiently localized in the model system, the effect of the low level region, $E^{\text{ES, low}}_{\text{real}} - E^{\text{ES, low}}_{\text{model}}$, may be calculated using the ground state energies. This is convenient when the low-level method cannot be used for excited states, for example, with molecular mechanics methods. Therefore, an electronic excitation in an IMOMM (or QM/MM) calculation always reduces to the excitation in the QM region alone. When the excitation is not localized in the model system, we need to employ an IMOMO scheme with excited state methods for both the low and the high level. Now special care must be taken to ensure that the results correspond to the correct electronic configuration; all three subcalculations must represent the same excitation. Because IMOMO does not provide an integrated wave function, the physical nature of the excitation is not self-evident. One has to pay attention to electronic properties such as the transition moments and nonadiabatic coupling, to ensure correct excited states. So far this aspect has not been addressed in detail.

The first IMOMO study on excited states was reported by Froese, and considered the $S_0$, $T_1$, and $T_2$ states of a series of alkenes (cyclopentene and norbornene) and enones. The specific state was calculated for both the high and low level method, which is relatively straightforward because these electronic states are the lowest in each spin/space symmetry. Several IMOMO combinations were investigated for the $S_0 \rightarrow T_1$ adiabatic excitation of the alkenes with $C_2$ and $C_4$ models, while for the enones the $S_0 \rightarrow T_{1,2}$ adiabatic excitations were

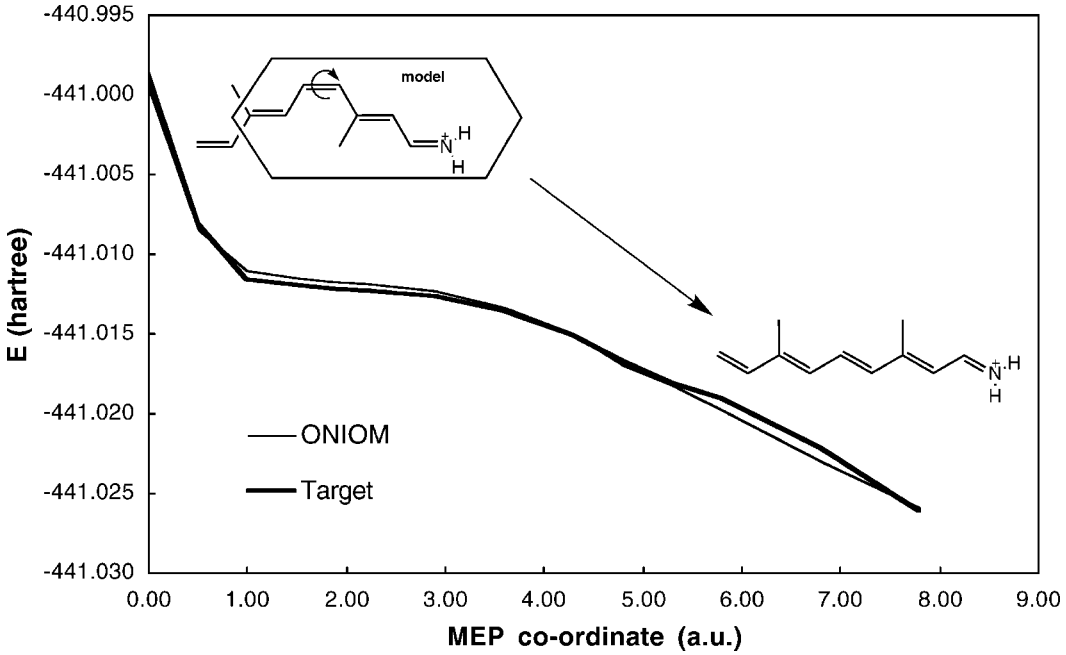


**FIGURE 4.** Target CASSCF$^{S1}$(10e/10o)/6-31G(d) and ONIOM(CASSCF$^{S1}$(8e,8o)/6-31G(d):UHF$^{T1}$/3-21G) curves for an $S_1$ photo isomerization path of a 11 non-H model for retinal protonated Schiff base.

investigated with acrolein as model. For the high level Froese used several high-correlation methods [MP2,3,4, CCSD(T), G2MS], and lower correlation methods for the low level (HF, MP2,3). The results show that the excitation energies are more sensitive to the high level method than the low level method. As expected, the $C_4$ model IMOMO calculation yields results closer to the target than the $C_2$ model calculation, but the differences are not large. The errors with the target are usually within several kcal/mol. These results suggest that the "triplet character" is localized in the model system, but this has not been investigated in detail.

Recently, we have applied IMOMO to the $S_1$ photoisomerization of retinal protonated Schiff base (PSB). As target we used an 11 non-H model for retinal PSB, calculated at the CASSCF(10e,10o)/6-31G(d). This is the system and the method Robb and Olivucci used to determine an isomerization reaction path on the $S_1$ potential energy surface,[38] which we attempted to reproduce using IMOMO. We tested several different partitionings, and a large number of methods for the low level, both including and excluding excited state methods. Surprisingly, the IMOMO(CASSCF$^{S1}$(8e,8o)/6-31G(d):UHF$^{T1}$/3-21G) combination, with an eight non-H model, yielded the best results. This is because the $T_1$ state has essentially the same electronic configuration as the $S_1$ state. Of course, as stand-alone method UHF$^{T1}$ would not reproduce the target well, but as a low-level method it reproduces the effects of low-level region on CASSCF quite well. In Figure 4 we show the energies of both the target and the ONIOM calculations along the minimum energy path (MEP) determined by CASSCF(10e,10o)/6-31G(d), starting at zero degrees and ending at a 68 degrees torsion angle. We find that the IMOMO error is clearly very small. One could argue that the model system is not significantly smaller (three non-H) than the real system, but the present ONIOM calculation costs only 10% of the CPU time required for CASSCF(10e,10o). More importantly, we can easily extend our systems to the full retinal PSB.

The ONIOM3(MO:MO:MM) method available in the Gaussian package provides an interesting option for large (biological) molecules in which the excitation is not confined to a region small enough to be treated at the highest computational level. In this scheme, the intermediate MO level can be employed for the less important delocalization, while still a very accurate method can be used for the part of the system in which most of the excitation is localized. We expect ONIOM3(MO:MO:MM) to be very useful for the study of light sensitive biological molecules, and intend to study the bacteriorhodopsin molecule with aforementioned IMOMO(CAS:HF) combina-

tion for the retinal fragment, augmented with an appropriate molecular mechanics method for the protein environment.

## Properties

An attractive feature of the IMOMO method is that integrated one-electron properties can also be calculated using the same extrapolation scheme. The expressions have are given in ref. 16, and are very similar to those for the integrated energy and its geometrical derivatives. The integration of mixed electric field and geometrical parameter derivatives provides important quantities such as infrared and Raman intensities.

Karadakov and Morokuma published the IMOMO calculation of NMR chemical shift.[39] The elements of a 3 × 3 shielding tensor for a nucleus can be written as

$$\sigma_{ab} = \left( \frac{\partial^2 E}{\partial B_a \partial \mu_b} \right), \tag{9}$$

where $B$ and $\mu$ are the nuclear magnetic moment and external magnetic field, respectively, and $a$ and $b$ denote the axes. When the isotropic shielding is required, the tensor does not need to be diagonalized, and the integrated nuclear shielding constant can be calculated with an expression analagous to the energy expression [eq. (1)].

$$\sigma_{\text{iso}}^{\text{IMOMO}} = \sigma_{\text{iso}}^{\text{low, real}} - \sigma_{\text{iso}}^{\text{low, model}} + \sigma_{\text{iso}}^{\text{high, model}} \tag{10}$$

When the anisotropic shielding is computed, one must first integrate the tensor, followed by the diagonalization and calculation of the shielding constants (note that the present Gaussian implementation diagonalizes individual subcalculation tensors, where one cannot simply add the individually diagonalized tensors). About the same time as Karadakov and Morokuma published the IMOMO study on the calculation of NMR chemical shifts, Cui and Karplus presented the calculation of these properties using their QM/MM method, in which the QM wave function is allowed to be polarized by the charge distribution in the MM region.[40]

Karadakov calculated the isotropic shielding for several systems (water dimer, ethanol, acetone, acrolein, fluorobenzene, and naphthalene) at the conventional (target) MP2-GIAO level, and using IMOMO(MP2-GIAO:HF-GIAO) [following eq. (10)]. Several partitionings were investigated, including some that are particularly challenging, for example cutting resonance structures. Therefore, not all the IMOMO results agree satisfactory with the target values, but the potential is clearly demonstrated. In Table V we show the calculated values for the water dimer (Fig. 5), in which either one of the water molecules can be treated at the high level. The largest deviation of the IMOMO results with the target MP2 results is 1.93 ppm, while the largest difference between the non-integrated HF and MP2 values is 15.24 ppm.

**TABLE V.**
**Isotropic NMR Chemical Shielding (ppm) for the Water Dimer (Fig. 5), Calculated at the Nonintegrated HF and MP2 Levels, and the Integrated MP2:HF Level, with the 6-31G* Basis Set.**

| | MP2 | HF | MP2:HF |
|---|---|---|---|
| $^{17}$O(1) | 355.41 | 342.82 (12.59) | 357.34 (1.93) |
| $^{1}$H(2) | 28.72 | 28.29 (0.43) | 28.72 (0.00) |
| $^{1}$H(3) | 32.02 | 31.68 (0.34) | 32.00 (0.02) |
| $^{17}$O(4) | 346.94 | 331.70 (15.24) | 346.17 (0.77) |
| $^{1}$H(5,6) | 30.77 | 30.47 (0.30) | 30.79 (0.02) |

Two different partitionings were employed in the IMOMO calculations: to calculate the shielding for atoms 1, 2, and 3, the water molecule consisting of these atoms was treated at the high level. To calculate the shielding for atoms 4, 5, and 6, the water molecule consisting of atoms 4, 5, and 6 was treated at the high level. The absolute differences of the HF or IMOMO calculation with the target MP2 calculation are given in parentheses.

## Other Work

Apart from our own studies, the IMOMO method has been used by several other groups. We already discussed the work by Truhlar and Coitiño on IMOMO bond dissociation energies and geometry optimization,[24–26] which was the result of a collaboration with Morokuma on the IMOMO scheme. Humbel, who was involved with the development of the IMOMO method,[10,21] later studied electron transfer processes in small molecules.[41] Especially since ONIOM became available in the Gaussian package, a number of articles have appeared from

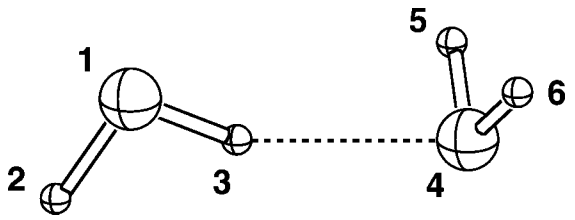


**FIGURE 5.** Water dimer.

groups who applied the method to their specific research interests. We will only briefly mention these studies.

Truong and Truong studied a series of hydrogen abstraction reactions of small (substituted) hydrocarbons at the IMOMO(MP4:BHLYP) level, employing a minimal model.[42] The reaction energies as well as the barrier heights were computed. The authors assessed the performance of IMOMO for these reactions, and the deviation from the target was usually within 1 kcal/mol. However, in several cases involving $\pi$-bond systems the error is larger. This article served as a preliminary study for the application of IMOMO in the study of kinetics of large systems using variational transition state theory.[43] Several other groups applied the ONIOM method, but did not provide a thorough investigation of the validity of the particular ONIOM combinations. Bruice and Kahn used IMOMO(MP2:HF) to study the enzyme active site of catechol O-methyltransferase (COMT),[44] which is a good example of partitioning the system into amino acid residues that are directly involved with the reaction, and residues that only play a supporting role. Goldfuss and coworkers studied large organic systems with HF, DFT, and MP2 methods for the high level, combined with the semiempirical AM1 in the low level.[45] In a separate study, Goldfuss used ONIOM(HF:UFF) for the investigation of organometallic systems.[46] Finally, Zimmerman reported structures of organic systems optimized using the ONIOM method, but did not give details of the partitioning or methods involved.[47]

## Conclusions and Future Developments

The IMOMO method, a version of the ONIOM method, can combine different levels of MO methods into a single integrated calculation of the energy or other electronic properties, a unique feature not available in other hybrid methods. The method elegantly takes into account both electronic and steric effects of the environment or substituents on the energy, geometry, and other properties of interest, and can be applied to excited states, as well as the ground state. The method is so flexible that the final choice of method and model combinations is entirely left to the user, who can tune it to be within the tolerated error (compared to either target calculations of experimental data) for the property under investigation. Generally speaking, if the target level is CCSD(T) or G2, the best choice of low level is MP2. If MP2 or DFT is the target level, HF or eventually semiempirical MO methods are good choices of low level.

Of course, ONIOM is not magic, and when the user fails to select the correct partitioning and method combination, the results can be very wrong. In the present work we have mainly reported results where ONIOM was used in the correct way, but in the articles that are referred to we often show the path that leads to the correct ONIOM combination, which includes many combinations that do not work. However, in virtually all cases we eventually found an ONIOM combination that yields acceptable results. This is expected, because ONIOM should converge to the "target" with the increased size of the model system, or the improvment of the method used for the low level. Only in cases where there is not a "main player" for the properties of interest in the system, as in example of the relative stability of $HCl(H_2O)_4$ complexes, the ONIOM method may not be suitable. One can verify the reliability of a perspective combination easily by performing the *S*-value test.

Possible future developments include the incorporation of the ONIOM method in the polarized continuum model for solvation.[48] A particularly interesting application of ONIOM+PCM would be to explicitly include several solvent molecules at the low level, as a buffer between the high level layer and the continuum. The effects of localized interaction of the solute with the first solvation shell will then be explicitly considered, and the effects of the continuum on the solute will be less prone to errors.

Furthermore, so far we have only explored potential energy surfaces in a static manner, but ONIOM can be used for other types of investigation as well. For example, we could perform direct dynamics calculations for large molecular systems using ONIOM energies and geometrical derivatives.[49] ONIOM energies and gradients can be obtained much cheaper than standard MO calculations for the same accuracy, and can be used to follow reaction dynamics of complicated molecular systems. In fact, any type of investigation of potential energy surfaces that can be carried out with conventional methods can be used with ONIOM as well.

## Acknowledgments

The authors are grateful to the past and present members of the Morokuma group, who contributed to the development and applications of the IMOMM, IMOMO, and ONIOM methods.

## References


1. Pople, J. A.; Head–Gordon, M.; Raghavachari, K. J Chem Phys 1987, 87, 5968.
2. Curtiss, L. A.; Raghavachari, K.; Trucks, G. W.; Pople, J. A. J Chem Phys 1991, 94, 7221.
3. Montgomery, J. A.; Ochterski, J. W.; Petersson, G. A. J Chem Phys 1994, 101, 5900.
4. Scuseria, G. E. J Phys Chem A 1999, 103, 4782.
5. Labanowski, J. K.; Andzelm, J. W., Eds. Density Functional Methods in Chemistry; Springer-Verlag: New York, 1991.
6. Saeb, S.; Pulay, P. Annu Rev Phys Chem 1993, 44, 213.
7. Gao, J. In Reviews in Computational Chemistry; Lipkowitz, K. B.; Boyd, D. B., Eds.; VCH: New York, 1996, p. 119, vol. 7.
8. Allinger, N. L. MM3(92); Quantum Chemistry Program Exchange; Bloomington, IN, 1992.
9. Maseras, F.; Morokuma, K. J Comput Chem 1995, 16, 1170.
10. Humbel, S.; Sieber, S.; Morokuma, K. J Chem Phys 1996, 16, 1959.
11. Svensson, M.; Humbel, S.; Froese, R. D. J.; Matsubara, T.; Sieber, S.; Morokuma, K. J Phys Chem 1996, 100, 19357.
12. Frisch, M. J.; Trucks, G. W.; Schlegel, H. B.; Scuseria, G. E.; Robb, M. A.; Cheeseman, J. R.; Zakrzewski, V. G.; Montgomery, J. A., Jr.; Stratmann, R. E.; Burant, J. C.; Dapprich, S.; Millam, J. M.; Daniels, A. D.; Kudin, K. N.; Strain, M. C.; Farkas, O.; Tomasi, J.; Barone, V.; Cossi, M.; Cammi, R.; Mennucci, B.; Pomelli, C.; Adamo, C.; Clifford, S.; Ochterski, J.; Petersson, G. A.; Ayala, P. Y.; Cui, Q.; Morokuma, K.; Malick, D. K.; Rabuck, A. D.; Raghavachari, K.; Foresman, J. B.; Cioslowski, J.; Ortiz, J. V.; Stefanov, B. B.; Liu, G.; Liashenko, A.; Piskorz, P.; Komaromi, I.; Gomperts, R.; Martin, R. L.; Fox, D. J.; Keith, T.; Al-Laham, M. A.; Peng, C. Y.; Nanayakkara, A.; Gonzalez, C.; Challacombe, M.; Gill, P. M. W.; Johnson, B.; Chen, W.; Wong, M. W.; Andres, J. L.; Gonzalez, C.; Head–Gordon, M.; Replogle, E. S.; Pople, J. A. Gaussian 98, Revision A.1; Gaussian, Inc.: Pittsburgh, PA, 1998.
13. http://euch4m.chem.emory.edu.
14. Maseras, F. Top Organomet Chem 1999, 4, 165.
15. Froese, R. D. J.; Morokuma, K. In The Encyclopedia of Computational Chemistry; Schleyer, P. v. R.; Allinger, N. L.; Clark, T.; Gasteiger, J.; Kollman, P. A.; Schaefer, H. F., III; Schreiner, P. R., Eds.; John Wiley: Chichester, 1998, p. 1245.
16. Dapprich, S.; Komáromi, I.; Byun, K. S.; Morokuma, K.; Frisch, M. J. J Mol Struct (Theochem) 1999, 461–462, 1.
17. Koga, N.; Morokuma, K. Chem Phys Lett 1990, 172, 243.
18. Gao, J.; Amara, P.; Alhambra, C.; Gield, M. J. J Phys Chem A 1998, 102, 4714.
19. Bersuker, I. B.; Leong, M. K.; Boggs, J. E.; Pearlman, R. S. Int J Quantum Chem 1997, 63, 1051.
20. Antes, I.; Thiel, W. J Phys Chem A 1999, 103, 9290.
21. Svensson, M.; Humbel, S.; Morokuma, K. J Chem Phys 1996, 105, 3654.
22. Bakowies, D.; Thiel, W. J Phys Chem 1996, 100, 10580.
23. Corchado, J. C.; Truhlar, D. G. J Phys Chem A 1998, 102, 1895.
24. Coitiño, E. L.; Truhlar, D. G. J Phys Chem A 1997, 101, 4641.
25. Noland, M.; Coitiño, E. L.; Truhlar, D. G. J Phys Chem A 1997, 101, 1193.
26. Coitiño, E. L.; Truhlar, D. G.; Morokuma, K. Chem Phys Lett 1996, 259, 159.
27. Froese, R. D. J.; Morokuma, K. J Phys Chem A 1999, 103, 4580.
28. Froese, R. D. J.; Morokuma, K. Chem Phys Lett 1999, 305, 419.
29. Vreven, T.; Morokuma, K. J Chem Phys 1999, 111, 8799.
30. Vreven, T.; Morokuma, K. in preperation.
31. Froese, R. D. J.; Humbel, S.; Svensson, M.; Morokuma, K. J Phys Chem A 1997, 101, 227.
32. McBride, J. M. Tetrahedron 1974, 30, 2009.
33. Froese, R. D. J.; Coxon, J. M.; West, S. C.; Morokuma, K. J Org Chem 1997, 62, 6991.
34. Coxon, J. M.; Froese, R. D. J.; Ganguly, B.; Marchand, A. P.; Morokuma, K. Synlett 1999, 11, 1681.
35. Re, S.; Osamura, Y.; Morokuma, K. in preparation.
36. Froese, R. D. J.; Morokuma, K. Chem Phys Lett 1996, 263, 393.
37. Vreven, T.; Morokuma, K. J Chem Phys 2000, 113, 2969.
38. Garavelli, M.; Vreven, T.; Celani, P.; Bernardi, F.; Robb, M. A.; Olivucci, M. J Am Chem Soc 1998, 120, 1285.
39. Karadakov, P. B.; Morokuma, K. Chem Phys Lett 2000, 317, 589.
40. Cui, Q.; Karplus, M. J Phys Chem B 2000, 104, 3721.
41. Humbel, S. J Mol Struct (Theochem) 1999, 461–462, 153.
42. Truong, T. N.; Truong, T.-T. T. Chem Phys Lett 1999, 314, 529.
43. Truong, T. N.; Maity, D. K.; Truong, T.-T. T. J Chem Phys 2000, 112, 24.
44. Kahn, K.; Bruice, T. C. J Am Chem Soc 2000, 122, 46.
45. Goldfuss, B.; Rominger, F. Tetrahedron 2000, 56, 881.
46. Goldfuss, B.; Steigelmann, M.; Khan, S. I.; Houk, K. N. J Org Chem 2000, 65, 77.
47. Zimmerman, H. E.; Alabugin, I. V.; Chen, W.; Zhu, Z. J Am Chem Soc 1999, 121, 11930.
48. Amovilli, C.; Barone, V.; Cammi, R.; Cancés, E.; Cossi, M.; Mennucci, B.; Pomelli, C. S.; Tomasi, J. Adv Quantum Chem 1999, 32, 227.
49. Chen, W.; Hase, W. L.; Schlegel, H. B. Chem Phys Lett 1994, 228, 436.